

Uni-Traveling-Carrier Photodiodes with Increased Output Response and Low Intermodulation Distortion

Jonathan Klamkin¹, Anand Ramaswamy², Yu-Chia Chang², Leif A. Johansson², Matthew M. Dummer²,
John E. Bowers², Steven P. DenBaars^{1,2}, Larry A. Coldren^{1,2}

1. Materials Department, University of California, Santa Barbara, CA 93106 USA

2. Electrical and Computer Engineering Department, University of California, Santa Barbara, CA 93106 USA

Email: klamkin@engineering.ucsb.edu

Abstract—Waveguide uni-traveling-carrier photodiodes have been fabricated and tested to investigate the influence of the doping profile in several of the device layers on saturation characteristics and linearity. Two particular photodiode (PD) structures are discussed. Compared to PD A, PD B has a lower and more graded p-doping profile in the absorber layer and also a higher n-doping level in the collector layer. For PD B a higher field is induced in the absorber layer and the higher doping in the collector layer provides charge compensation. An enhancement in the response for PD B is observed with increasing photocurrent. At a frequency of 1 GHz the saturation current for PD A is 65 mA and that for PD B is 63 mA. The third-order intermodulation distortion was also measured at various photocurrent levels. For PD A, the third-order output intercept point (OIP3) for photocurrent levels of 10 mA, 20 mA, and 30 mA is 34.7 dBm, 38.6 dBm, and 35.8 dBm respectively. Those for PD B are 28.1 dBm, 41.0 dBm, and 37.2 dBm. These are all for a bias of -5 V. While PD A has a higher OIP3 at lower photocurrent levels, PD B is favorable for high current operation.

I. INTRODUCTION

To improve signal-to-noise ratio and spur-free dynamic range in analog fiber-optic links, a novel coherent receiver architecture has been proposed requiring photodetectors that have high saturation current and high linearity at GHz frequencies [1]. The uni-traveling-carrier photodiode (UTC-PD) demonstrates both high speed and high current operation [2]. In a UTC-PD light is absorbed in an undepleted p-type narrow bandgap layer (absorber) and photogenerated electrons subsequently diffuse to a wide bandgap drift layer (collector). Because electrons are the only active carriers and electrons have a higher drift velocity than holes, space charge saturation effects should be reduced when compared to a traditional PIN photodiode (PD). Several techniques for improving the performance of UTC-PDs have been demonstrated. Charge compensation was used to improve the saturation current by intentionally n-doping the collector layer [3]. By doing so, the electric field is preconditioned to be higher in the presence of a large mobile space charge density. Others have reported an enhancement in the response of UTC-PDs that have a graded doping profile in the p-type absorber [4]. This grade results in a potential profile that can aid electron

transport. This same effect was also observed for UTC-PDs with uniform but relatively lower absorber doping [5]. We previously reported waveguide UTC-PDs that demonstrated output saturation currents greater than 40 mA at 1 GHz and a third-order output intercept point (OIP3) of 43 dBm at 20 mA and 34 dBm at 40 mA [6]. Here we have closely investigated the effects of the doping profile in several layers of UTC-PDs on the output response, saturation current, and third-order intermodulation distortion (IMD3). In particular, two different waveguide UTC-PDs were fabricated and characterized. The most significant differences in these devices are the doping profiles within the absorber and collector layers. The devices are referred to as PD A and PD B. For PD A, the p-doping in the absorber layer is not only higher, but also more uniform. The n-doping in the collector layer is lower in PD A at around $7E15 \text{ cm}^{-3}$ whereas for PD B it is around $6E16 \text{ cm}^{-3}$. For PD B an enhancement in the output response is observed at high current. This is believed to be due to the combination of the lower and more graded absorber doping profile as well as the higher collector doping level. The lower and more graded doping level in the absorber results in a small field induced at high current levels, and the higher collector doping level provides charge compensation. Both PDs exhibit very high saturation current levels that, to the best of our knowledge, are some of the highest reported for waveguide photodiodes at comparable frequencies. Due to the response enhancement with increasing photocurrent for PD B, the OIP3 increases with photocurrent more so than for PD A. Therefore PD B exhibits higher linearity at high photocurrent levels.

II. DEVICE DESIGN AND FABRICATION

The PD structures are grown directly above an InGaAsP optical waveguide. Passive regions are formed by selectively removing the PD layers. This is followed by a blanket InP cladding and InGaAs contact layer regrowth. The layer structure following regrowth is shown in Table 1. The p-doping level in the absorber and the n-doping level in the collector are denoted P and N respectively. The doping levels for those layers which are unintentionally doped are denoted UID. The n-InP field termination layer terminates the applied field across

TABLE I
UTC-PD LAYER STRUCTURE

| Layer | Thickness (nm) | Doping (cm^{-3}) |
|--------------------------|----------------|-----------------------------|
| p-InGaAs contact | 150 | $2\text{E}19$ |
| p-InP cladding | 2,000 | $1\text{E}18$ |
| p-InGaAs absorber | 75 | P |
| InGaAs | 8 | UID |
| InGaAsP | 16 | UID |
| InP | 6 | UID |
| n-InP | 7 | $1\text{E}18$ |
| n-InP collector | 200 | N |
| n-InP field termination | 25 | $2\text{E}18$ |

the collector layer of the PD in the photodetection regions and prevents depletion of the optical waveguide below. Light is coupled into the optical waveguide in a passive region and then absorbed as it passes through a photodetection region. Because of the spatial separation of the absorber layer in the UTC-PD structure and the peak of the incoming optical mode, carrier generation is distributed more uniformly along the length of the device. This as well as a wide input waveguide help to reduce front-end saturation. Of particular interest are the doping profiles in the absorber layer and collector layer. The absorber p-doping level was intended to be greater than $2\text{E}18 \text{ cm}^{-3}$. Zn, which is used as the p-dopant, diffuses readily during growth therefore the grading in the doping profile can vary. For PD B, the absorber peak doping level is around 25% lower than that for PD A, and the profile is more graded (high to low) toward the absorber/collector interface. The n-doping in the collector layer is also nearly an order of magnitude higher for PD B at around $6\text{E}16 \text{ cm}^{-3}$. This doping level is adequate for providing charge compensation. Devices were fabricated with various geometries. The results that follow are for devices that are $10 \mu\text{m}$ wide and $150 \mu\text{m}$ long.

III. RESULTS AND DISCUSSION

The electrical frequency response of the UTC-PDs was measured at various biases for photocurrent levels up to around 70 mA. Fig. 1 shows the normalized RF power as a function of DC photocurrent at 1 GHz for both devices. For PD A, the response is fairly constant with photocurrent until the onset of saturation. For PD B, there is a significant enhancement in the response with increasing photocurrent. This enhancement is due in part to a small field induced in the absorber at high photocurrent levels. The p-doping in the absorber of PD B is lower and more graded so this field should be greater in this device. The enhancement could also be due to the higher n-doping in the collector of PD B. This doping provides some charge compensation and preconditions the electric field for operation at high photocurrent levels. The saturation current, defined here as the photocurrent level where the RF response decreases by 1 dB, is around 65 mA for PD A and around 63 mA for PD B for biases of around -3.5 V. Because the device areas are large, the 3-dB bandwidth is RC-limited. Therefore any enhancement in the response should be attributed more so to improvements in the field distribution in the depletion region or the capacitance of the device rather than improvements

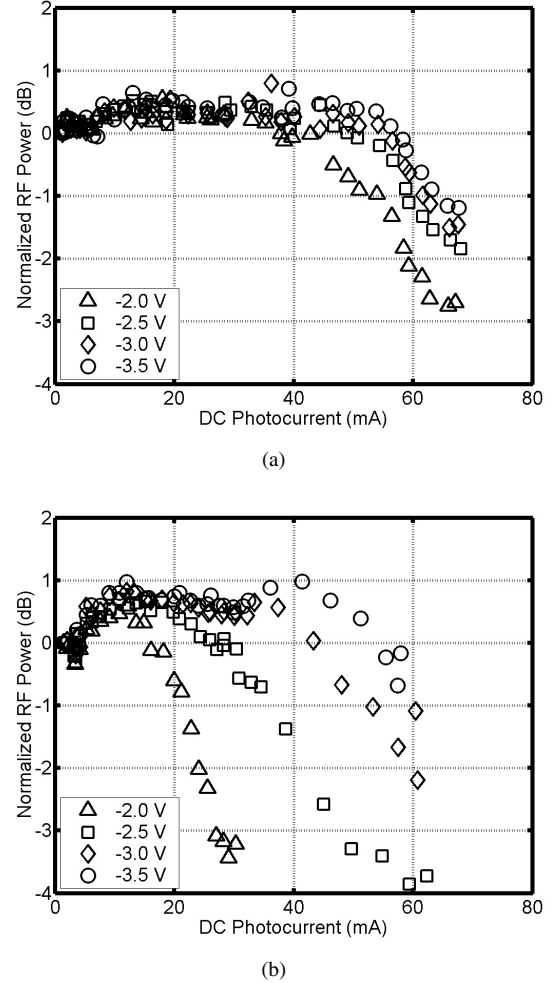
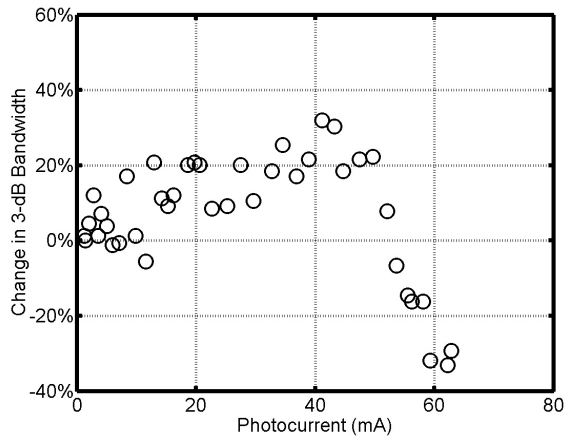
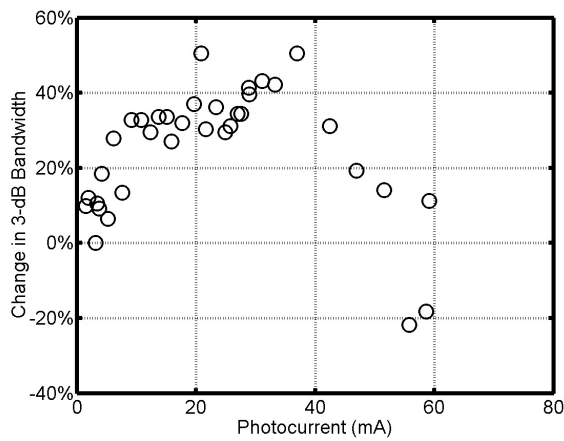


Fig. 1. Normalized RF power as a function of DC photocurrent at 1 GHz for (a) PD A and for (b) PD B.

in carrier transit time. The change in 3-dB bandwidth as a function of DC photocurrent level is shown in Fig. 2 for both PDs. At 1 mA the 3-dB bandwidth of PD A is 2.2 GHz and that for PD B is 1.6 GHz. As expected, there is a larger enhancement with increasing photocurrent for PD B. For this PD the 3-dB bandwidth is enhanced by as much as 40-50% whereas for PD A it is enhanced by at most around 30%. The saturation current was also extracted at 0.5 GHz and 2 GHz. For PD A, the saturation current at these frequencies is 67 mA and 62 mA respectively. For PD B it is 60 mA and 62 mA. To characterize the linearity of the PDs, a two-tone setup was used. Tones were generated at 1 GHz and 0.8 GHz. The output fundamental and IMD3 power were measured as a function of input modulation power at various photocurrent levels and biases. Fig. 3 shows the results of the IMD3 measurements at 10 mA and 20 mA for both UTC-PDs. For these measurements the bias for both devices was -5 V. For PD A, the measured OIP3 was 34.7 dBm and 38.6 dBm for photocurrent levels of 10 mA and 20 mA respectively. For PD B the OIP3 was 28.1 dBm and 41.0 dBm at the



(a)



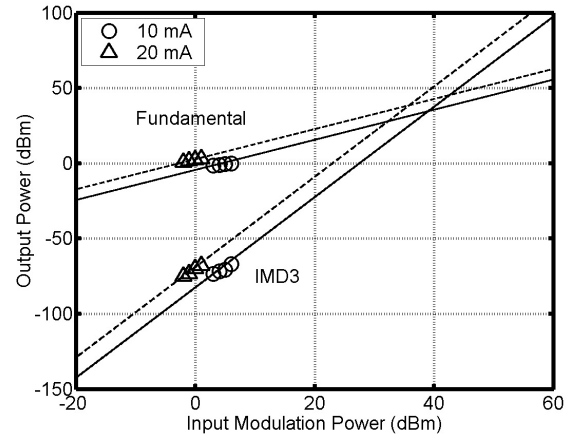
(b)

Fig. 2. Change in 3-dB bandwidth as a function of DC photocurrent for (a) PD A and for (b) PD B. The bias is -3.5 V for both devices.

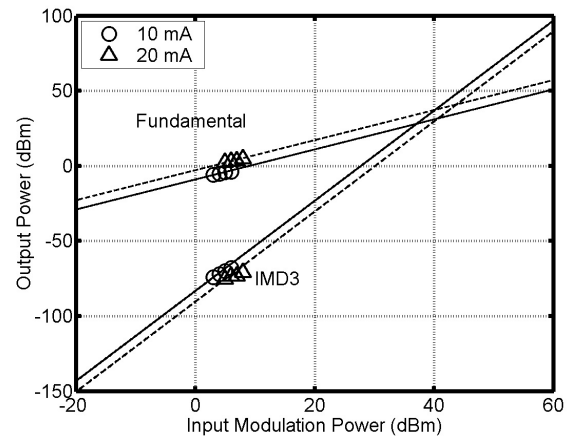
same photocurrent levels. Although the OIP3 improves with increasing photocurrent for both devices, this improvement is far greater for PD B. Fig. 4 shows the IMD3 measurements for both devices at a photocurrent level of 30 mA and a bias of -5 V. The OIP3 at these conditions for PD A is 35.8 dBm and that for PD B is 37.2 dBm. The bias was kept constant at -5 V for these measurements to make a fair comparison. Increasing the bias improves the OIP3 for both PDs, however the maximum achievable OIP3 for photocurrent levels higher than 10 mA is greater for PD B. It appears that because of its enhanced response, this PD exhibits lower IMD3 at high photocurrent levels.

IV. CONCLUSIONS

We have fabricated and tested UTC-PDs with different absorber and collector layer doping profiles. An enhancement in the response is observed for PD B which has a lower and more graded absorber doping as well as a higher collector doping. These result in a higher induced field in the absorber layer and charge compensation respectively. Saturation currents of



(a)



(b)

Fig. 3. IMD3 measurements at 10 mA and 20 mA for (a) PD A and for (b) PD B. The bias is -5 V for both devices.

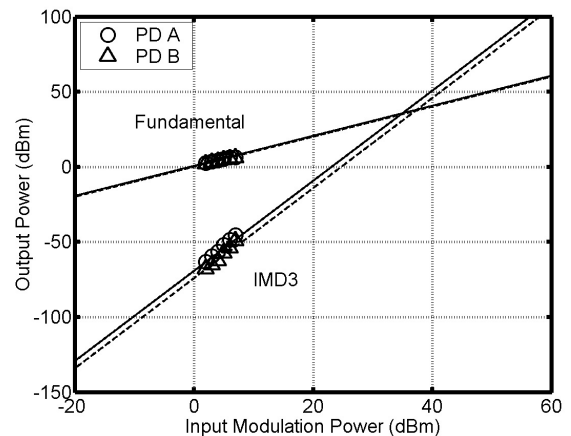


Fig. 4. IMD3 measurements at 30 mA for PD A and for PD B. The bias is -5 V for both devices.

65 mA for PD A and 63 mA for PD B are demonstrated. To the best of our knowledge these represent some of the highest saturation currents reported for waveguide PDs. IMD3 measurements were also performed to investigate the effects of the response enhancement observed for PD B on linearity. The OIP3 at photocurrent levels of 10 mA, 20 mA, and 30 mA was measured to be 34.7 dBm, 38.6 dBm, and 35.8 dBm for PD A and 28.1 dBm, 41.0 dBm, and 37.2 dBm for PD B. The linearity is better at high photocurrent levels for PD B therefore this PD is preferable for high current operation.

ACKNOWLEDGMENT

This research was supported by the DARPA PHOR-FRONT program under United States Air Force contract number FA8750-05-C-0265.

REFERENCES

- [1] A. Ramaswamy, L. A. Johansson, J. Klamkin, C. Sheldon, H.-F. Chou, M. J. Rodwell, L. A. Coldren, and J. E. Bowers, "Coherent receiver based on a broadband optical phase-lock loop," in *OFC Postdeadline Papers*, 2007.
- [2] T. Ishibashi, T. Furuta, H. Fushimi, S. Kodama, H. Ito, T. Nagatsuma, N. Shimizu, and Y. Miyamoto, "InP/InGaAs uni-traveling-carrier photodiodes," *IEICE Transactions on Electronics*, vol. E83-C, no. 6, pp. 938–949, June 2000.
- [3] N. Li, X. Li, S. Demiguel, X. Zheng, J. C. Campbell, D. A. Tulchinsky, K. J. Williams, T. D. Isshiki, G. S. Kinsey, and R. Sudharsanan, "High-saturation-current charge-compensated InGaAs-InP uni-traveling-carrier photodiode," *IEEE Photonics Technology Letters*, vol. 16, no. 3, pp. 864–866, March 2004.
- [4] N. Shimizu, N. Watanabe, T. Furuta, and T. Ishibashi, "InP-InGaAs uni-traveling-carrier photodiode with improved 3-dB bandwidth of over 150 GHz," *IEEE Photonics Technology Letters*, vol. 10, no. 3, pp. 412–414, March 1998.
- [5] N. Shimizu, N. Wantanabe, T. Furuta, and T. Ishibashi, "Improved response of uni-traveling-carrier photodiodes by carrier injection," *Japanese Journal of Applied Physics*, vol. 37, pp. 1424–1426, 1998.
- [6] J. Klamkin, A. Ramaswamy, L. A. Johansson, H.-F. Chou, M. N. Sysak, J. W. Raring, N. Parthasarathy, S. P. DenBaars, J. E. Bowers, and L. A. Coldren, "High output saturation and high-linearity uni-traveling-carrier waveguide photodiodes," *IEEE Photonics Technology Letters*, vol. 19, no. 3, pp. 149–151, February 2007.